Bottomonium production at forward rapidity with ALICE at the LHC

Massimiliano Marchisone
on behalf of the ALICE Collaboration

Università di Torino and INFN

The 2nd International Conference on
Initial Stages in High-Energy Nuclear Collisions
Napa, 03–07/12/2014

Outline

1. Bottomonia in hadron collisions
2. ALICE
3. pp results
4. Pb–Pb results
5. p–Pb results
6. Conclusions

Quarkonia in A-A and p-A collisions

- Quarkonia play an important role in the study of Quark-Gluon Plasma (a deconfined phase of nuclear matter) because:
  - they are created in the early stage of nucleus-nucleus collisions;
  - the production is expected to be modified by the QGP (PLB 178 (1986) 416);
  - having different radii (i.e. different binding energies) a sequential suppression is expected (PRD 64 (2001) 094015).
- Concurrent mechanisms may occur:
  - $c\bar{c}$ recombination is expected to be important for charmonium at LHC energy;
  - cold nuclear matter effects (shadowing and parton energy loss in particular) can modify quarkonium production even in absence of the hot and dense matter.
- The study of p-A collisions is therefore essential to disentangle the hot from the cold matter effects and to understand the results in A-A collisions.

The importance of bottomonium production

- The $Q\bar{Q}$ binding into quarkonium states is a non-perturbative process still not well understood $\rightarrow$ theoretical calculations for bottomonium production are more robust due to the higher mass of the b quark.
- The probability of Υ regeneration by $b\bar{b}$ recombination is much smaller than that for the the J/ψ ($\sim$ 100 $c\bar{c}$ pairs per central event w.r.t. a few $b\bar{b}$ pairs at LHC energy).
- The measurement of Υ in p-A collisions allows a study of CNM effects in a slightly different Bjorken-x range, complementing the J/ψ studies.

A Large Ion Collider Experiment

- ALICE is the LHC experiment dedicated to the study of ultrarelativistic heavy-ion collisions.
- It has also an interesting pp program.
- At forward rapidity ($2.5 < y < 4$) quarkonium states are reconstructed via the dimuon decay down to transverse momentum (p_T) equal to 0 with the **Muon Spectrometer**.

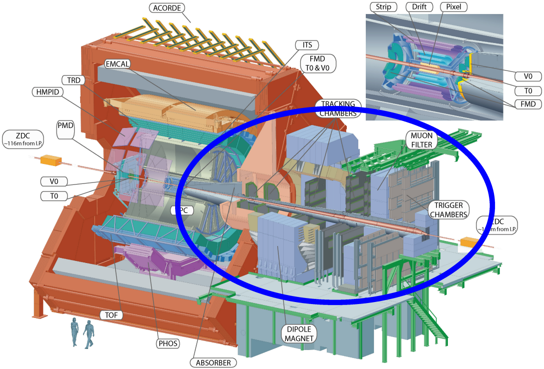

- V0 and T0 detectors are also used in the analyses for triggering purposes, while the SPD is used for primary vertex reconstruction.

Production cross sections in pp collisions at $\sqrt{s} = 7$ TeV

- The analysis is based on a data sample corresponding to an integrated luminosity of 1.35 pb^{-1} (EPJC 74 (2014) 2974).

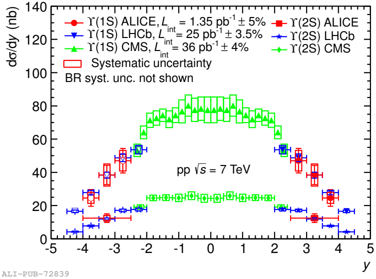

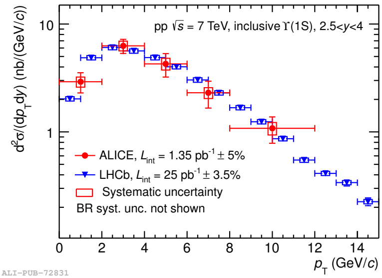

- The p_T and y-differential cross sections compared to the values reported by LHCb (EPJC 72 (2012) 2025) show a good agreement for both resonances. They complement the measurements performed by CMS at midrapidity.

Cross sections in pp collisions: model comparisons

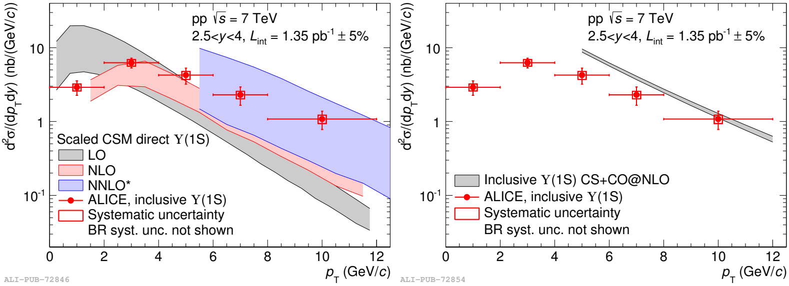

- CSM predictions are scaled by a factor 1/0.6 to account for the feed-down from $\Upsilon(2S)$, $\Upsilon(3S)$ and χ_b:
  - LO calculation underestimates the data for $p_T > 4$ GeV/c;
  - NLO calculation reproduces the data at low p_T, but it still underestimates the cross section over the full range;
  - a good agreement is achieved at NNLO*, over a limited p_T range and with large uncertainties.
- NRQCD (with feed-down) overestimates the data, but the disagreement becomes smaller at higher p_T.

$\Upsilon(1S)$ production in Pb–Pb collisions at $\sqrt{s_{NN}} = 2.76$ TeV

- The analysed data sample corresponds to an integrated luminosity of 69 μb^{-1} (PLB 738 (2014) 361-372).
- The in-medium modification is evaluated through the nuclear modification factor: $R_{AA} = \frac{Y_{AA}}{\langle T_{AA} \rangle \cdot \sigma_{pp}}$.

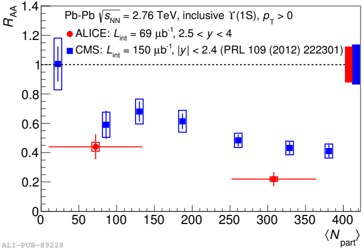

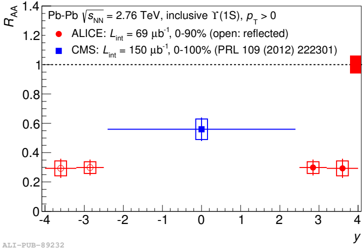

- The suppression increases with the centrality of the collisions.
- The value of the $\Upsilon(1S)$ R_{AA} in $2.5 < y < 4$ is significantly lower than the measurement made by CMS at midrapidity in $|y| < 2.4$ (PRL 109 (2012) 222301).

Comparison with a dynamical model

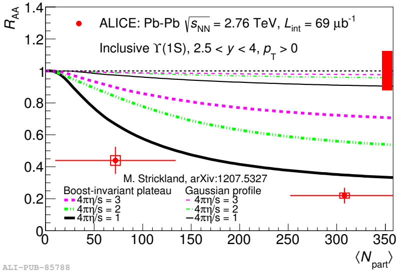

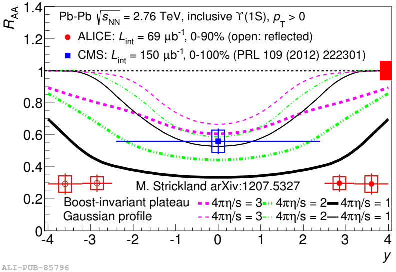

- The QGP is described by means of a dynamical model which includes the suppression of the different bottomonium states, but not CNM effects nor recombination.
- Two initial temperature rapidity profiles: boost-invariant plateau and Gaussian with 3 values of η/s for each of them.
- None of the calculations reproduce the ALICE data. The rapidity trend measured by ALICE and CMS is opposite to what predicted by the model.

Comparison with transport models

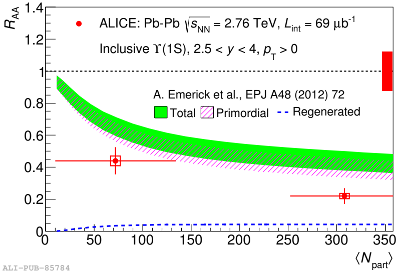

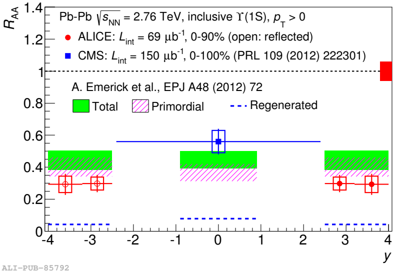

- The model accounts for both suppression and regeneration mechanisms.
- Cold nuclear matter effects are considered by means of an effective absorption cross section between 0 and 2 mb, including shadowing, nuclear absorption and Cronin effect.
- The measured R_{AA} is overestimated by the calculation that, however, reproduces the decreasing trend with $\langle N_{part} \rangle$. The model predicts an R_{AA} almost constant as a function of rapidity, not supported by the data.

Comparison with transport models

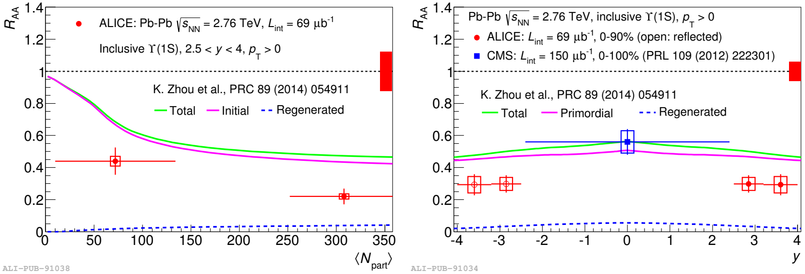

- The model includes Υ suppression, a small regeneration component and shadowing effects (EKS98 parametrization).
- Also in this case the calculations underestimate the observed suppression and fails to reproduce its rapidity dependence.
- A precise measurement of feed-down and CNM effects is therefore necessary in order to make a more stringent comparison with models.

Υ production in p–Pb collisions at $\sqrt{s_{NN}} = 5.02$ TeV

- The data set corresponds to an integrated luminosity of 5.0 nb^{-1} in p–Pb and 5.8 nb^{-1} in Pb–p collisions.

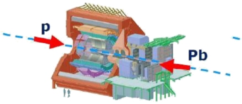

$2.03 < y_{CMS} < 3.53$

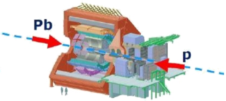

$-4.46 < y_{CMS} < -2.96$

- The CNM effects are quantified by the $\boxed{R_{pPb} = \frac{\sigma_{pPb}}{A_{Pb} \cdot \sigma_{pp}}}$.
- Results are available on PLB 740 (2015) 105-117.

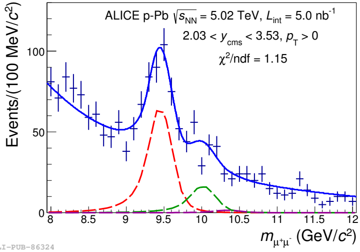

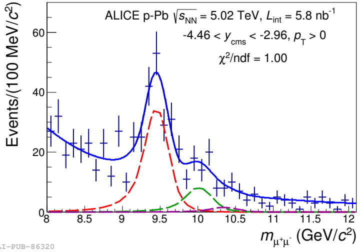

$\Upsilon(1S)$ R_{pPb} measurements

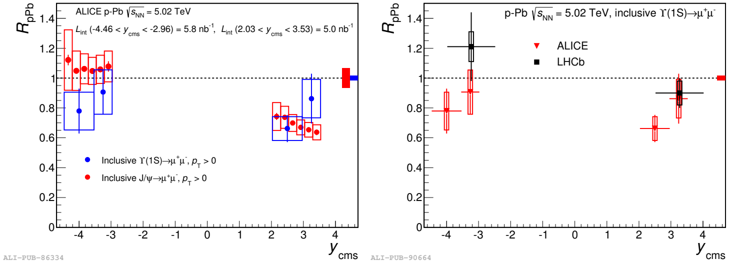

- The $\Upsilon(1S)$ is suppressed at forward rapidity, while at backward rapidity the R_{pPb} is compatible with unity within uncertainties, disfavouring a strong gluon anti-shadowing.
- At positive y_{cms} the $\Upsilon(1S)$ and J/ψ R_{pPb} are rather similar. At negative rapidity, the J/ψ R_{pPb} is systematically above that of $\Upsilon(1S)$, even if they are still consistent within uncertainties.
- The R_{pPb} measured by LHCb (JHEP 07 (2014) 094) is consistent within uncertainties with the ALICE result.

$\Upsilon(1S)$ $R_{\rm pPb}$ compared to theoretical models

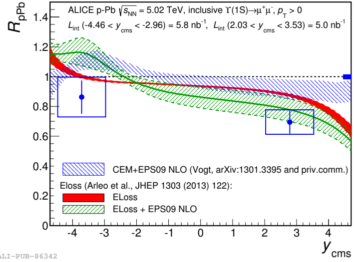

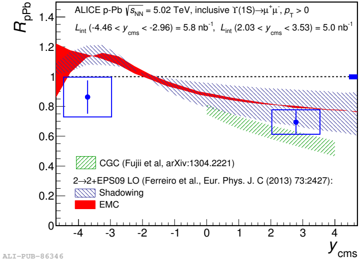

- NLO CEM calculation with EPS09 overestimates the measured $R_{\rm pPb}$.
- The parton energy loss with EPS09 calculation reproduces well the data at forward rapidity, while data at backward rapidity are in a better agreement with parton energy loss only calculation.
- In the framework of a $gg \to \Upsilon g$ model, the $R_{\rm pPb}$ at backward rapidity disfavours the strong gluon anti-shadowing included in the EPS09 parametrization.
- The calculation based on the CGC slightly underestimates the $R_{\rm pPb}$, but it is not able to reproduce the J/ψ measurements in the same rapidity range.

Forward-to-backward ratio (R_{FB})

- R_{FB} is the ratio of the nuclear modification factors at forward and at backward rapidities in a range symmetric with respect to $y_{cms} = 0$. It is independent of the pp cross section.

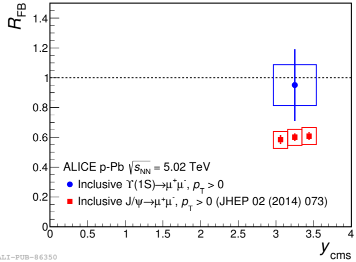

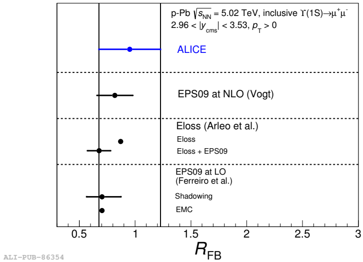

- In the rapidity range $2.96 < |y_{cms}| < 3.53$ the $\Upsilon(1S)$ R_{FB} is compatible with unity and is larger than that of the J/ψ.
- All models describe the data within the uncertainty of the measurement.

$\Upsilon(2S)$-to-$\Upsilon(1S)$ cross sections ratio

- The $\Upsilon(2S)$-to-$\Upsilon(1S)$ cross section ratio measured by ALICE in p–Pb collisions is:

$-4.46 < y_{\rm cms} < -2.96$	$0.26 \pm 0.09 \pm 0.04$
$2.03 < y_{\rm cms} < 3.53$	$0.27 \pm 0.08 \pm 0.04$

- The same ratio has been measured in pp collisions by ALICE at $\sqrt{s} = 7$ TeV[1] and by LHCb at various energies in the range $2.0 < y < 4.5$[2].

ALICE $\sqrt{s} = 7$ TeV	0.28 ± 0.08
LHCb $\sqrt{s} = 2.76$ TeV	0.24 ± 0.03
LHCb $\sqrt{s} = 7$ TeV	0.25 ± 0.02
LHCb $\sqrt{s} = 8$ TeV	0.23 ± 0.01

- The cross section ratio in p–Pb collisions measured by ALICE at forward rapidity is compatible with that for pp collisions: within uncertainties there is no evidence of a different magnitude of CNM effects between the two states.

[1] EPJC 74 (2014) 2974

[2] EPJC 72 (2012) 2025, EPJC 74 (2014) 2835, JHEP 1306 (2013) 064

Conclusions

pp collisions:

- the p_T and y-differential production cross sections are in good agreement with measurements by LHCb and complement the results at midrapidity from CMS;
- CSM calculations underestimate the data at large p_T. The leading-p_T NNLO helps to reduce the disagreement but with larger uncertainties.

Pb–Pb collisions:

- the observed $\Upsilon(1S)$ suppression is stronger in central than in semiperipheral collisions and shows a pronounced rapidity dependence over the large domain covered by ALICE and CMS;
- all models underestimate the suppression at forward rapidity.

p–Pb collisions:

- the $\Upsilon(1S)$ $R_{\rm pPb}$ is consistent with unity at backward rapidity suggesting a small gluon anti-shadowing;
- models tend to overestimate the measurements and cannot describe the full rapidity dependence.
- the $\Upsilon(2S)$-to-$\Upsilon(1S)$ ratio shows no evidence of different CNM effects on the two states.

Backup

Quarkonium production mechanisms /1

In hadron collisions the dominant processes involved in the quarkonium production are gluon fusion and gluon fragmentation.

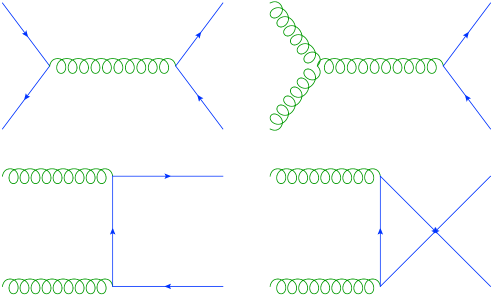

The creation of a pair $q\bar{q}$ pair can be calculated with a perturbative approach. This is not valid for the transition to the quarkonium state.

Quarkonium production mechanisms /2

- Color Singlet Model: the $q\bar{q}$ pair evolving in a quarkonium state is in a colour singlet state and the quantum numbers are conserved after the formation of the meson.
- Color Evaporation Model: the production rate for the quarkonium state is a certain fraction of the cross section for producing $q\bar{q}$ pairs. There are not constraints on the quantum numbers of the final state. The $q\bar{q}$ pair neutralizes its colour by interaction with the collision-induced colour field.
- Non-Relativistic QCD: the production cross section of a quarkonium state is written as a sum of terms taking into account a short distance partonic cross section and a long distance matrix element: $d\sigma(H) = \sum_n d\widehat{\sigma}\left(q\bar{q}_n\right)\langle 0|\mathcal{O}_n^H|0\rangle$.

Quarkonium in heavy-ion collisions

- Quarkonia play an important role in the study of Quark-Gluon Plasma (a deconfined phase of quarks and gluons) because:
  - they are created in the early stage of the collision;
  - the production is expected to be modified by the QGP (PLB, 178 (1986) 416);

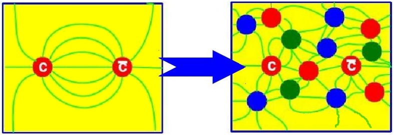

  - having different radii (i.e. different binding energies) a sequential suppression is expected (PRD, 64 (2001) 094015).
- Concurrent mechanisms:
  - an important $c\bar{c}$ recombination is expected at LHC energy;
  - cold nuclear matter (CNM) effects can modify quarkonium production even in absence of hot and dense matter.

Quarkonium regeneration

Quarkonium regeneration is due to the statistical recombination of the heavy quarks emerging from the medium. It is more and more important when the center-of-mass energy of the collision increases.

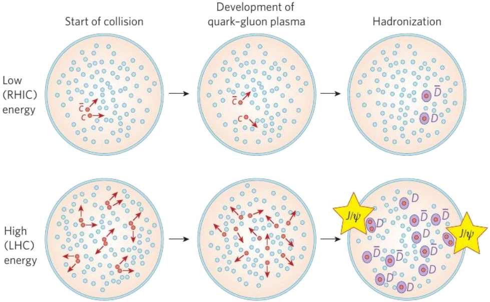

Accelerator and center-of-mass energy	SPS 20 GeV	RHIC 200 GeV	LHC 2.76 TeV
$N_{c\bar{c}}$/event	~ 0.2	~ 10	~ 60
$N_{b\bar{b}}$/event	–	~ 0.05	~ 6

CNM effects: shadowing

PDF of a nucleon in a nucleus $\neq$ PDF of a free nucleon.

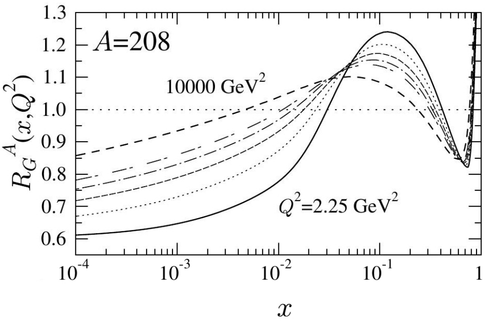

Plot shows the ratio between the gluon PDF in a nucleon of a Pb nucleus and in a free proton as a function of the Bjorken-x (from EPS09 model).

The quarkonium cross sections ($\Rightarrow$ the yields) depend on PDF. Therefore their modifications influence the comparison of the different collision systems even in absence of QGP.

Shadowing and Bjorken region

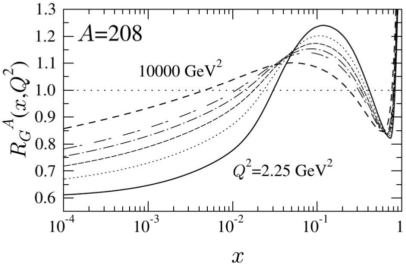

Shadowing: $x_{\mathrm{Bj}} < 0.01$, anti-shadowing: $0.01 < x_{\mathrm{Bj}} < 0.3$; EMC effect: $0.3 < x_{\mathrm{Bj}} < 0.7$; Fermi motion: $x_{\mathrm{Bj}} > 0.7$.

Under the assumption of the $gg \rightarrow \Upsilon$ production process, the sampled Bjorken-x are:

- $5.5 \cdot 10^{-5} < x_{\mathrm{Bj}} < 2.5 \cdot 10^{-4}$ (shadowing region) at forward rapidity;
- $3.6 \cdot 10^{-2} < x_{\mathrm{Bj}} < 1.6 \cdot 10^{-1}$ (anti-shadowing region) at backward rapidity.

Bjorken-x range

- Assuming a 2→1 production process the tested Bjorken-x ranges are
  - Backward: $3.6\cdot10^{-2} < x < 1.6\cdot10^{-1}$ (Υ) and $1.2\cdot10^{-2} < x < 5.3\cdot10^{-2}$ (J/ψ)
  - Forward: $5.5\cdot10^{-5} < x < 2.5\cdot10^{-4}$ (Υ) and $1.8\cdot10^{-5} < x < 8.1\cdot10^{-5}$ (J/ψ)

$$x_{1,2} = \frac{m_T}{\sqrt{s}} \cdot e^{\pm y}$$

CNM effects: coherent parton energy loss and Cronin effect

- Coherent parton energy loss: a parton moving through the nucleus can scatter elastically and lose energy before the hard scattering. The effect is responsible of an hadrons suppression in pA collisions.
- Cronin effect: a parton can undergo a multiple scattering process in the nucleus before to hadronize. It acquires an extra transverse momentum which modifies the p_T spectrum of the hadrons with respect to pp collisions. This effect is responsible of an enhanced hadron production in pA collisions.

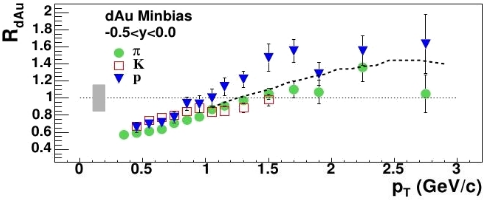

CNM effects: nuclear and comovers absorption

This final state effect is responsible of the break-up of the quarkonium state. It occurs when the $q\bar{q}$ pair is formed and passes through the nucleus and is parametrized using a phenomenological production cross section:

$$\sigma(AB \to J/\psi) \propto ABe^{-\rho\sigma_{abs}L}$$

A and B are the mass numbers of the nuclei, ρ is the nuclear density, L is the path length of the pair through the nuclear matter and σ_{abs} is the absorption cross section which decreases increasing the collision energy.

Similarly, in a dense gas system formed by conventional hadrons like pions and kaons, the quarkonium could be suppressed by processes like $J/\psi + \pi \to D + \bar{D} + X$, called suppression by hadronic comovers.

The ALICE Muon Spectrometer

The Muon Spectrometer is composed of:

- front absorber;
- beam shield;
- iron wall;
- dipole (integrated field = 3 T·m);
- muon tracking chambers (10 planes of MWPC with a spatial resolution in the bending coordinate better than 100 μm);
- muon trigger chambers (4 planes of RPC with a time resolution of some ns and the possibility to deliver single and dimuon triggers above two p_T cuts).

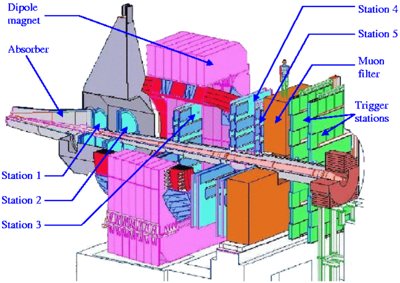

Invariant mass spectra

pp collisions

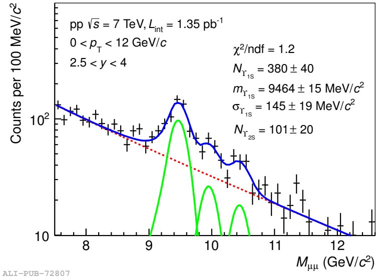

Pb–Pb collisions

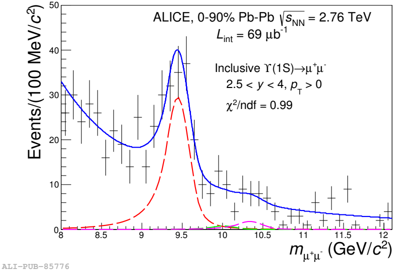

Systematics on $\Upsilon(1S)$ R_{AA}

Source	**Value (%)**
Cross section in pp	7–25
Normalization (CMUL $\rightarrow$ MB)	2
Signal extraction	5–10
Trigger efficiency	2
Tracking efficiency	7–9
Matching efficiency	1
MC inputs	5

Systematics on Υ cross section in pp collisions

Source	Value (%)
Luminosity	5
Signal extraction	8–13
Trigger efficiency	3
Tracking efficiency	5–10
Matching efficiency	1
MC inputs	0.6–4.5

Dynamical model

- The prediction is based on a complex potential approach in an evolving QGP described by an hydrodynamics formalism. The imaginary part is related to the in medium decay.
- The boost invariant plateau describing the spatial temperature profiles corresponds to a Bjorken picture (transparency in collisions), a Gaussian profile corresponds to a Landau picture (colliding nuclei lose all their energy).
- The plasma shear viscosities $4\pi\eta/s = \{1, 2, 3\}$ corresponds to different initial temperatures $T_0 = \{520, 504, 494\}$ MeV in central collisions, in order to keep $dN_{ch}/dy = 1400$ fixed.
- The suppression of direct $\Upsilon(1S)$ is $\sim 50\%$ of the total R_{AA}.
- Since CNM effects are not included in the model, the predictions should be considered as an upper limit.
- This model describes successfully the elliptic flow of charged particles measured by ALICE in Pb–Pb collisions at $\sqrt{s_{NN}} = 2.76$ TeV.

Transport model

- Model relies on a strongly binding scenario $\rightarrow$ the suppression of the $\Upsilon(1S)$ is small, while that of higher states is substantial.
- The suppression and regeneration contributions are balanced by means of a rate equation: $\boxed{\frac{dN_\Upsilon}{dt} = -\Gamma_\Upsilon^{diss}(N_\Upsilon - N_\Upsilon^{eq})}$.
- The spatio-temporal evolution of the medium is described by an expanding fire cylinder whose initial dimension are tuned according to the recent LHC measurements.
- The initial condition for the number of bottomonia at the QGP formation time and the implemented regeneration component requires the knowledge of the beauty quark cross-section.
- The CNM considered (shadowing, Cronin effect and energy loss) are approximated by a suppression factor: $e^{-\rho\sigma_{abs}L}$, from Glauber model and previous measurements.

Nuclear modification factor

$$R_{AA} = \frac{Y^{AA}_{\Upsilon(1S)}}{\underbrace{\langle N_{coll} \rangle}_{\langle T_{AA} \rangle \cdot \sigma_{N-N}} \cdot Y^{pp}_{\Upsilon(1S)}} =$$

$$= \frac{Y^{AA}_{\Upsilon(1S)}}{\langle T_{AA} \rangle \cdot \underbrace{\sigma_{N-N} \cdot Y^{pp}_{\Upsilon(1S)}}_{\sigma^{pp}_{\Upsilon(1S)}}} =$$

$$= \frac{Y^{AA}_{\Upsilon(1S)}}{\langle T_{AA} \rangle \cdot \sigma^{pp}_{\Upsilon(1S)}}$$

Old reference cross section

Up to a few months ago, the reference cross section in pp collisions at 2.76 TeV in the ALICE kinematic domain was estimated as follows:

- interpolation of cross section data at various energy by different experiments (CDF, D0 and CMS) at midrapidity, plus the use of the FONLL predictions based on CEM;
- extrapolation of the previous result at forward rapidity with Pythia in the bins of the analysis.

Preliminary results relied on this approach.

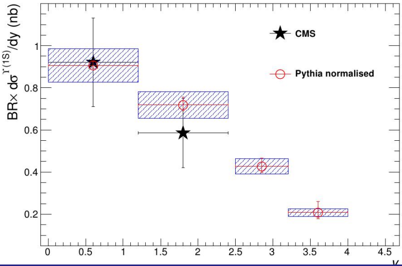

Rapidity	σ_{pp} (nb) value±extrap.±norm.
$2.5 < y < 3.2$	$12.05^{+9\%}_{-7\%} \pm 9\%$
$3.2 < y < 4$	$6.71^{+25\%}_{-14\%} \pm 9\%$

New reference cross section

- Then, LHCb published the Υ cross section measurements in pp collisions at 2.76 TeV at forward rapidity: we used their values to get a cross section in our bin.

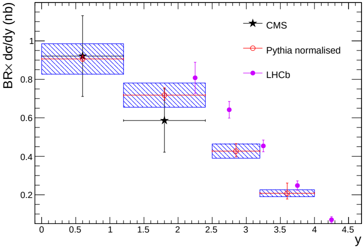

Rapidity	$\sigma^{pp}_{\Upsilon(1S)} \pm \text{uncorr} \pm \text{corr}$ (nb)
$2.5 < y < 3.2$	$16.93 \pm 0.73 \pm 0.60$
$3.2 < y < 4$	$10.20 \pm 0.64 \pm 0.36$

- The results obtained with the old method underestimate the LHCb measurements (difference of 30–35%, not recovered by uncertainties): it reflects into a decrease of the R_{AA} modifying all the conclusions made in the preliminary results.

New reference cross section

- A few months ago LHCb published the Υ cross section measurements in pp collisions at 2.76 TeV at forward rapidity.
- Since their rapidity bins don't correspond to ours, we fitted their differential values to different symmetric functions and then we integrated the results according to our bins.

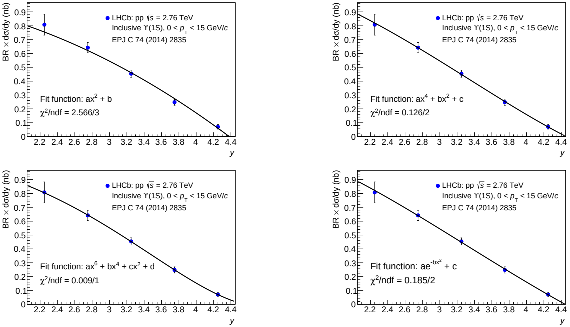

Comparison with ALICE J/ψ at forward rapidity

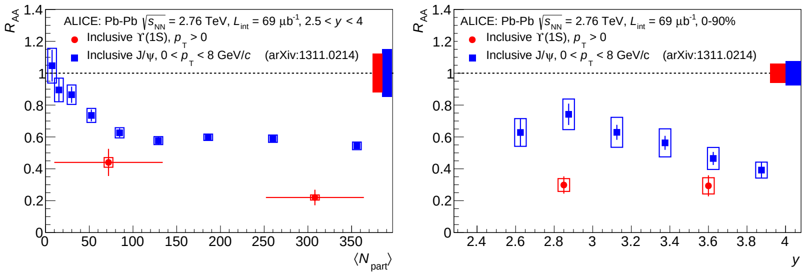

- The R_{AA} is about two times larger for J/ψ than for $\Upsilon(1S)$ in central collisions, while the results are closer for semiperipheral ones.
- $\Upsilon(1S)$ is more suppressed than J/ψ even versus rapidity.
- It is difficult to make conclusions due to the different contribution of regeneration and feed-down from higher mass states for and $\Upsilon(1S)$.

Systematics on $\Upsilon(1S)$ R_{pA}

Source	Backward rapidities	Forward rapidities
Signal extraction: $\Upsilon(1S)$	5%-6%(II)	4%-6%(II)
Signal extraction: $\Upsilon(2S)$	12%(II)	12%(II)
Input MC parameterization: $\Upsilon(1S)$	2%-5%(II)	4%-6%(II)
Input MC parameterization: $\Upsilon(2S)$	5%(II)	5%(II)
Tracking efficiency	6%(II)	4%(II)
Trigger efficiency	2%(II)	2%(II)
Matching efficiency	1%(II)	1%(II)
$\sigma_{pp}^{\Upsilon(1S)}$ (interpolation)	11%-13% (II)	7%-12%(II)
$\mathscr{L}$ (correlated)	1.6%(I)	1.6%(I)
$\mathscr{L}$ (uncorrelated)	2.7%(II)	2.9%(II)

p–Pb and Pb–p collisions: energy and rapidity

- $\sqrt{s_{NN}} = 5.02$ TeV in nucleon-nucleon center of mass
  - p beam energy: 4 TeV
  - Pb beam energy: 1.58 TeV/A
  - $\Rightarrow \Delta y_{NN} = 0.465$ in p beam direction
- p–Pb collisions: $2.03 < y_{cms} < 3.53 \Rightarrow 3.43 < y_{lab} < 4$
- Pb–p collisions: $-4.46 < y_{cms} < -2.96 \Rightarrow 2.5 < y_{lab} < 3.07$
- Rapidity overlap region: $2.96 < |y_{cms}| < 3.53$

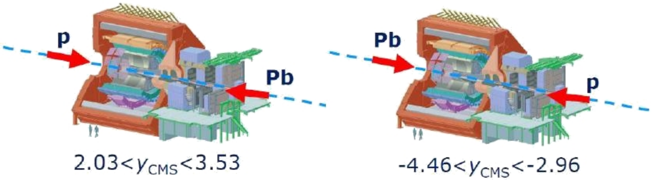

Υ differential cross sections in p–Pb collisions

$$\sigma_{\mathrm{pPb}}^{\Upsilon(1S)}(-4.46 < y_{\mathrm{cms}} < -2.96) = 5.57 \pm 0.72(\mathrm{stat}) \pm 0.57(\mathrm{syst})\ \mu\mathrm{b}$$

$$\sigma_{\mathrm{pPb}}^{\Upsilon(1S)}(2.03 < y_{\mathrm{cms}} < 3.53) = 8.45 \pm 0.94(\mathrm{stat}) \pm 0.75(\mathrm{syst})\ \mu\mathrm{b}.$$

$$\sigma_{\mathrm{pPb}}^{\Upsilon(2S)}(-4.46 < y_{\mathrm{cms}} < -2.96) = 1.85 \pm 0.61(\mathrm{stat}) \pm 0.33(\mathrm{syst})\ \mu\mathrm{b}$$

$$\sigma_{\mathrm{pPb}}^{\Upsilon(2S)}(2.03 < y_{\mathrm{cms}} < 3.53) = 2.97 \pm 0.82(\mathrm{stat}) \pm 0.50(\mathrm{syst})\ \mu\mathrm{b}.$$

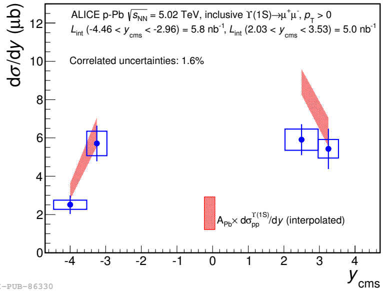

- The red bands correspond to the interpolated inclusive $\Upsilon(1S)$ pp cross section multiplied by the Pb mass number (208).
- $\sigma_{\mathbf{pp}}^{\Upsilon(1S)}$ at 5.02 TeV is evaluated interpolating LHCb data at 2.76, 7 and 8 TeV (provided in $2 < y < 4.5$) in our y-bins.
- For each rapidity bin, the cross section as a function of energy was fitted according to different shapes based on LO–CEM, FONLL and on phenomenological functions (ALICE-PUBLIC-2014-002).
- The final values were averaged together.